Dissipative effects in spallation-induced fission of ^{208}Pb at high excitation energies

Y. Ayyad,[1] J. Benlliure,[1,*] J. L. Rodríguez-Sánchez,[1] A. Bacquias,[2] A. Boudard,[3] E. Casarejos,[1,†] T. Enqvist,[4] M. Fernandez,[1] V. Henzl,[2] V. Henzlova,[2] B. Jurado,[5] A. Kelić-Heil,[2] T. Kurtukian,[5] S. Lukić,[2] P. Nadtochy,[2] D. Pérez-Loureiro,[1] R. Pleskač,[2] F. Farget,[6] M. V. Ricciardi,[2] K.-H. Schmidt,[2] C. Schmitt,[6] and Son Nguyen Ngoc[2]

[1]*Universidade de Santiago de Compostela, E-15758 Santiago de Compostela, Spain*
[2]*GSI, Helmholtzzentrum für Schwerionenforschung GmbH, D-64941 Darmstadt, Germany*
[3]*CEA-Saclay/IRFU, 91191 Gif-sur-Ivette, France*
[4]*Oulu southern Institute and Department of Physics, University of Oulu, Finland*
[5]*CENBG, CNRS/IN2P3, Université de Bordeaux, F-33175 Gradignan, France*
[6]*GANIL, BP 55027, F-14076 Caen Cedex 05, France*

(Received 4 December 2014; published 2 March 2015)

Spallation reactions on fissile nuclei represent an appropriate tool to investigate dissipative effects in nuclear fission. In this work, we have studied transient and dissipative effects in proton- and deuteron-induced fission on ^{208}Pb at 500A MeV. A dedicated experimental setup optimized for inverse kinematics measurements made it possible to identify in atomic number both fission fragments with high resolution, and reconstruct the charge of the fissioning system. We could then determine the width of the fission fragments charge distribution as well as partial fission cross sections, both as a function of the charge of the fissioning system. These two complementary observables permitted us to investigate the dynamics of the process at small deformation, i.e., from the ground state to the saddle point. The description of these observables with advanced model calculations reveals the influence of the nuclear dissipation in the fission process at high excitation energy and in particular its manifestation through transient time effects.

DOI: 10.1103/PhysRevC.91.034601 PACS number(s): 25.40.Sc, 25.85.Ge

I. INTRODUCTION

Spallation reactions are an important tool to investigate the dynamics of the fission process at low deformation owing to the high excitation energy, small shape distortion, and angular momentum induced into the fissioning system. Fission can be understood as a diffusion process over the barrier that needs a certain time to reach a quasistationary equilibrium [1]. This diffusion process is often described using transport models (Langevin or Fokker-Planck equations) [2] in terms of the evolution of a set of macroscopic collective coordinates, in interaction with a heat bath defined by the remaining intrinsic degrees of freedom. It is generally accepted that from ground-state deformation to scission, the evolution of the system is governed by the nuclear potential, the inertia tensor, and the reduced dissipation coefficient β, that defines the rate of the energy exchange between collective and intrinsic degrees of freedom.

A direct consequence of this dynamical picture of fission with respect to statistical models is a reduction of the fission width and a delay of the process characterized by a given transient time [3]. Because of the relatively short value of the transient time deduced until now (of the order of 10^{-21} s) [4–7], transient time effects manifest at high excitation energy where their magnitude is comparable to typical statistical lifetimes of the fissioning nuclei. At low excitation energy transient effects are then negligible and the fission rate is mainly ruled by the available phase space over the barrier.

The most clear evidence of dissipative and transient effects in fission was the failure of the statistical model [8] in reproducing prescission neutron multiplicities [9]. Nevertheless, after important efforts invested in understanding the dynamics of the fission process at high excitation energy, the magnitude of the dissipation strength and the transient time, together with their possible dependencies on the temperature and the deformation of the fissioning nuclei, is still controversial and not fully understood [4,5,7,10–13].

Fission dynamics has been extensively investigated in heavy compound nuclei by means of fusion-fission reactions [4,5,10]. In such reactions, the compound nucleus is characterized by a broad angular momentum spectrum and relatively low excitation energy which may hinder the manifestation of dynamical effects. Moreover, the compound nucleus is formed following a complex shape evolution starting from the contact of two colliding nuclei that may also end in quasifission [14]. Many different observables such as evaporation residue and fission cross sections [10], cumulative fission probabilities [15], or γ-ray [16] and light particle multiplicities [17] have been exploited to investigate the effect of the nuclear dissipation in fusion-fission reactions.

Spallation [18–21] and fragmentation [6,7] reactions have also been used to study the dynamics of the fission process. Spallation reactions are usually described as a two-step process involving an intranuclear cascade and a subsequent evaporation stage [22]. The interaction between the projectile and the target nuclei leads to a thermalized compound nucleus at the end of the cascade stage, referred to as a prefragment. In reactions induced by protons with relativistic energies, prefragments are typically produced with an average excitation energy of few hundreds of MeV spanning a broad distribution,

*Corresponding author: j.benlliure@usc.es
†Present address: Universidade de Vigo, E-36310 Vigo, Spain.

relatively low angular momentum, up to $10-20\ \hbar$, and with shapes close to the ones of the initial target nuclei [23,24]. These reactions thus fulfill the conditions proposed by Grangé and collaborators [3,25] for the manifestation of transient effects in fission.

Generally, conventional spallation-fission experiments are performed in direct kinematics [26–29] where the identification of the fission fragments in atomic number is a difficult task and only long-lived target materials can be studied. To overcome these difficulties, the inverse kinematics technique is better suited to unambiguously identify the products of the reaction. In this case heavy nuclei are accelerated up to relativistic energies and impinge onto light targets, usually proton or deuterium. Due to the kinematics of the reaction, all products are emitted in the forward direction with large kinetic energies and can be easily detected and identified.

Isotopic yields of spallation-evaporation residues and fission fragments were first proposed as observables for the investigation of dissipative and transient effects in spallation-induced fission reactions investigated in inverse kinematics [19,20]. However, these works already pointed to the need of additional observables to constrain the different parameters affecting the determination of the fission width in model calculations.

Following this suggestion, Jurado and collaborators proposed to investigate dissipative and transient effects from the characteristics of the final fission fragments, in particular their charge distribution [6]. In this experiment, the setup [30] provided the identification in atomic number of the two fragments produced in fission reactions induced by ^{238}U projectiles impinging onto a CH_2 target. Two new observables were then proposed, the distribution of partial fission cross sections and the width of the charge distributions of the fission fragments, both as a function of the sum of the charges of the two fragments. The latter was previously proposed in Ref. [20] over the integral charge distribution. These two observables provided unambiguous indication on the role of dissipative and transient effects in fission at high excitation energy [6].

A few years later, in Refs. [7,31] it was shown that the quantitative values of the dissipation strength and transient time obtained by Jurado and collaborators were affected by the initial deformation of the fissioning nuclei that were investigated. Therefore a new experiment was proposed by Schmitt and collaborators based on the same experimental setup but investigating the fission of nearly spherical radioactive fissioning systems produced by fragmentation. In this case dissipative and transient effects could be determined although only the width of the charge distribution of the fission fragments was used as an observable [7].

In the present work we revisited these two last experiments, using a different reaction mechanism and profiting also from the best conditions and observables. We investigate proton- and deuteron-induced fission of ^{208}Pb at $500A$ MeV in inverse kinematics using also an experimental setup providing the identification in atomic number of both fission fragments. This allows us to study the fission of nearly spherical fissioning systems with high excitation energy and low angular momentum. Moreover, we could use the two observables that were proposed to better constrain model calculations describing the dynamical evolution of the fissioning system from the ground state to the saddle point. The two targets used in this experiment also allowed us to cover two different overlapping ranges in excitation energy.

II. EXPERIMENT

A detailed description of the experimental setup and the determination of the total fission cross sections for the reactions $^{208}\mathrm{Pb} + p$ and $^{208}\mathrm{Pb} + d$ at $500A$ MeV were presented in a previous publication [32]. For these two reactions, total fission cross sections of 146 ± 7 mb and 203 ± 9 mb were obtained, respectively. The value of the total fission cross section obtained with protons is in very good agreement with a recent measurement yielding 149 ± 8 mb [33]. In this paper we will briefly recall the experimental setup and we will focus on the technique used to determine of the atomic number of the fission fragments (Z_1, Z_2) to obtain the partial fission cross sections and the width of the fission fragments charge distribution as a function of the charge of the fissioning system.

To produce compound nuclei with suited conditions to investigate transient effects in fission [3], the experiment was conducted at the GSI accelerator facility. A primary beam of ^{208}Pb was accelerated at $500A$ MeV by the SIS-18 synchrotron and guided to the setup for fission measurements (Fig. 1). The ^{208}Pb beam impinged onto a target cell with 100 μm titanium windows, containing liquid hydrogen (85 g/cm^2) or liquid deuterium (201 g/cm^2). A plastic scintillator detector (Start) placed upstream of the target was used to trigger the data acquisition. Two multisampling ionization chambers (MUSIC 1 and 2) with 200×80 mm^2 window surface and 460 mm of active length surrounded the target to identify reactions of ^{208}Pb beam particles in other layers of matter placed along the beam line. The first MUSIC chamber was also used to determine the number of projectiles which was of the order of 10^3 ions/s. Owing to the kinematics of the reaction, both fission fragments were emitted in forward direction with high kinetic energy. A double ionization chamber (Twin MUSIC) placed downstream of the second MUSIC detected both fission fragments in coincidence and allowed an unambiguous determination of both atomic numbers Z_1 and Z_2. In order to calibrate the vertical position of the fragments inside the

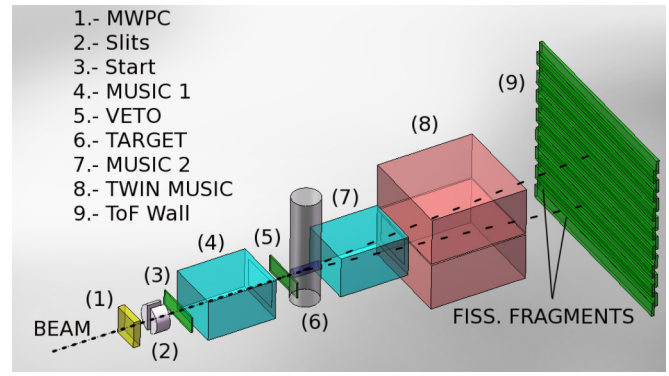

FIG. 1. (Color online) Schematic representation of the experimental setup used in the present experiment.

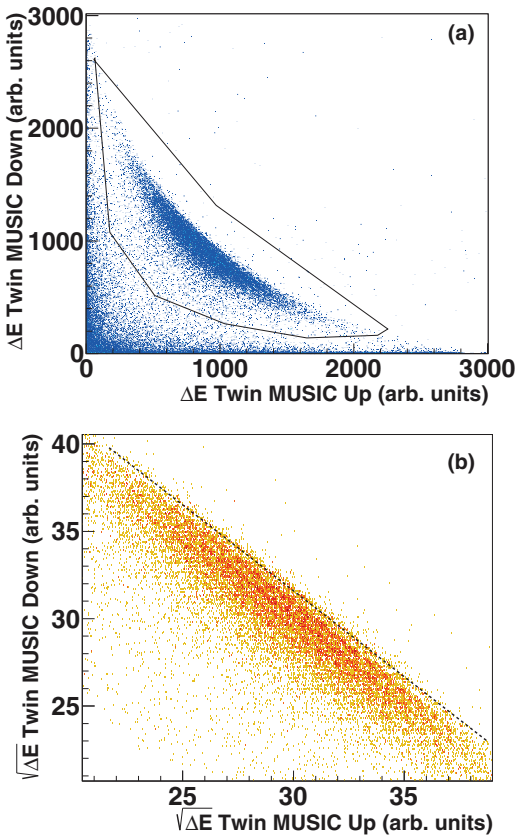

FIG. 2. (Color online) Upper panel: Scatter plot of the energy loss of the fission fragments recorded in each Twin MUSIC part. The contour (solid line) encloses the selected fission events. Lower panel: Same as upper panel but for the square root of the energy loss. Events with $Z_1 + Z_2 = 83$ are located around the dashed line.

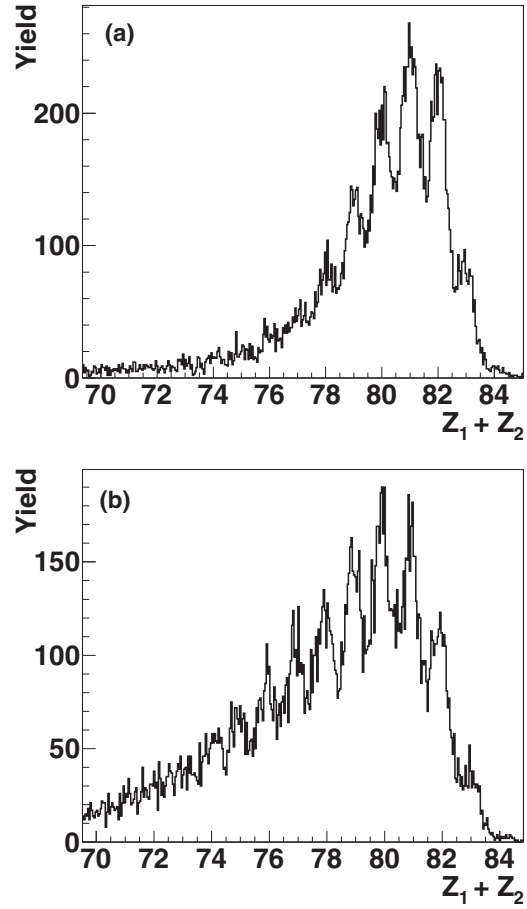

FIG. 3. Sum spectrum of fission fragments nuclear charge $Z_1 + Z_2$ for the ^{208}Pb + p (upper panel) and ^{208}Pb + d (lower panel) reactions at 500A MeV.

Twin MUSIC to deduce its efficiency, a time-of-flight wall (ToF Wall) composed of plastic scintillators was installed downstream of the chamber.

Fission events were selected using the energy loss of the fission fragments in each part of the Twin MUSIC detector as shown in the scatter plot of the upper panel in Fig. 2. Both parts of this chamber were calibrated separately in atomic number. This calibration was made assuming that the energy loss of the fission fragments in each part of the Twin-MUSIC is proportional to their atomic number squared, as shown in the lower panel in Fig. 2. It can be clearly seen that there exists a linear correlation between the square root of the energy-loss signals registered in both parts of the Twin MUSIC. The sum of the square root of the energy loss signals corresponds to the nuclear charge of the fissioning system, assuming no proton evaporation from the fission fragments.

According to this, the sum spectra provide the absolute calibration in atomic number of the fission fragments $Z_1 + Z_2$, as shown in Fig. 3 for the reactions ^{208}Pb + p (upper panel) and ^{208}Pb + d (lower panel). In these spectra, the peak with the largest value of $Z_1 + Z_2$ corresponds to projectiles undergoing double (n,p) charge-exchange reactions $Z = Z_1 + Z_2 = 84$ while the adjacent peak on the left corresponds to the single charge-exchange (n,p) of the projectile nuclei $Z = Z_1 + Z_2 = 83$. These charge-exchange processes can be mediated by the exchange of a virtual pion between the colliding nucleons (quasielastic charge exchange) or the excitation of a nucleon resonance decaying by pion emission (inelastic charge exchange). In the single charge exchange producing $Z_1 + Z_2 = 83$ the process is governed by a single nucleon-nucleon charge exchange process, elastic or inelastic. For the double charge exchange at least two nucleon-nucleon charge-exchange collisions are required. These results are consistent with charge-pickup reactions investigated with a ^{208}Pb beam impinging in proton and deuterium targets at 1A GeV [34]. Moreover, intranuclear cascade codes describe rather well those reaction channels [35]. Finally, this $Z_1 + Z_2$ calibration is also consistent with other works where the nuclear charge of the fissioning system was measured for reactions of nuclei with similar fissility, such as ^{214}Ra + CH_2 at 420A MeV [36].

After the charge identification of the fissioning system in the $Z_1 + Z_2$ spectrum, we calibrated the charge distribution of each fission fragment by unambiguously assigning a value of atomic number to each peak constrained by the corresponding $Z_1 + Z_2$ value (see Fig. 4). The final charge distribution of the fission fragments shown in Fig. 4 was corrected by the detection efficiency of the experimental setup. The detection

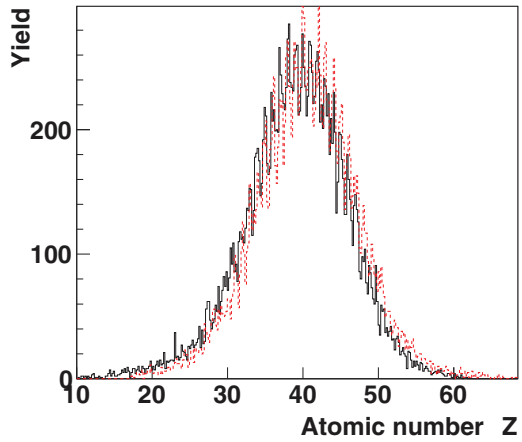

FIG. 4. (Color online) Calibrated fission fragment charge distributions recorded in both parts of the Twin MUSIC for the ^{208}Pb + p reaction. Solid and dashed lines refer to upper and lower parts of the Twin MUSIC, respectively.

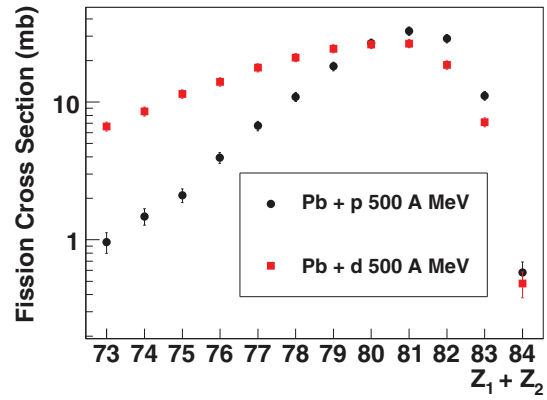

FIG. 5. (Color online) Partial fission cross sections as a function of the charge of the fissioning nucleus for the ^{208}Pb + p (circles) and ^{208}Pb + d (squares) reactions at 500A MeV.

efficiency was evaluated with a Monte Carlo simulation, taking into account the characteristics of the fission fragments (see Sec. III B), their kinematic properties, and the geometry of the detection setup. After applying this correction factor to the experimental distributions, the width of the charge distribution for the ^{208}Pb + p reaction amounts to $\sigma_z = 6.6 \pm 0.7$ charge units, while the mean value of the nuclear charge is 40.0 ± 0.5. These values are in rather good agreement with the ones obtained in Ref. [37] for the same reaction, $\sigma_z = 6.3 \pm 0.3$ and 40.0 ± 0.1 for the width and the mean value, respectively. Our results are also consistent with the ones obtained by Hagebø and Lund [38] for proton-induced fission of lead in direct kinematics at 600 MeV, $\sigma_z = 6.4$, and a mean value of 40.0 ± 0.1. For ^{208}Pb + d we obtained $\sigma_z = 7.0 \pm 0.5$ charge units and a mean value of 39.1 ± 0.5. The difference in the mean value of the charge distribution between reactions induced with protons and deuterons is explained by the larger excitation energy gained by the prefragments in the latter case.

III. RESULTS

A. Experimental observables

The size of the fissioning system, that we can approach from the sum of the charges of the two fission fragments $Z = Z_1 + Z_2$, can be used to assess the excitation energy imparted to the compound nuclei or prefragments produced in the spallation process [6,7]. The partial fission cross sections according to the different $Z_1 + Z_2$ values should then be a good observable to characterize the ground-to-saddle dynamics of the fission process.

In order to determine the partial fission cross sections as a function of the charge of the fissioning nucleus, the number of fission events for each $Z_1 + Z_2$ value was extracted from the two-dimensional scatter plot of the square root of the energy loss signal of both fission fragments (lower panel of Fig. 2). As can be seen, each line defined by the data in the experimental spectrum corresponds to one $Z_1 + Z_2$ value, where the dashed line indicates $Z_1 + Z_2 = 83$. The values of the partial fission cross sections were obtained by applying the same correction factors considered for the determination of the total fission cross section reported in Ref. [32] (geometrical efficiency, beam attenuation, and secondary reactions of the fission fragments in the target), but in this case according to the charge of the fissioning nucleus.

Partial fission cross sections for proton- and deuteron-induced fission of ^{208}Pb are shown in Fig. 5. As mentioned, the difference between the number of protons of the ^{208}Pb projectiles and the fissioning nuclei after spallation is related to the impact parameter and excitation energy induced in the reaction. Therefore, the smaller values of $Z_1 + Z_2$ correspond to the more violent collisions and vice versa. In addition, the fissility of the fissioning system (Z^2/A) decreases with $Z_1 + Z_2$, consequently the partial fission cross section is a function of this parameter and the excitation energy. One can see that in the case of the deuteron-induced reaction we obtain higher cross sections for the lower values of $Z_1 + Z_2$ with respect to the case of the proton-induced reaction. This can be attributed to the fact that deuterons induce higher excitation energies in the system because the total kinetic energy of the reaction is a factor 2 larger than the one corresponding to protons [39].

Conversely, for the largest values of $Z_1 + Z_2$ (above 80), where low excitation energies are expected, partial fission cross sections are slightly larger in reactions induced by protons. A possible explanation relies on the impact parameter because for the most peripheral collisions, only one of the nucleons of the deuterium will impact with the lead nuclei. Recently, a total fission cross section for the n + $^{\text{nat}}$Pb reaction at 500 MeV of 97 ± 7 mb was reported [40], which is a factor 1.5 smaller than the one obtained in [32] for protons. This could explain the reduction of the partial fission cross section in deuteron-induced fission for the largest impact parameters.

To illustrate the different ranges in excitation energy covered with the two targets we performed calculations with nuclear-reaction codes (See Sec. III B). As can be seen in Fig. 6, the distribution of excitation energy of all prefragments produced in deuteron-induced spallation of ^{208}Pb (dotted line) covers a larger range in excitation energy than the one obtained

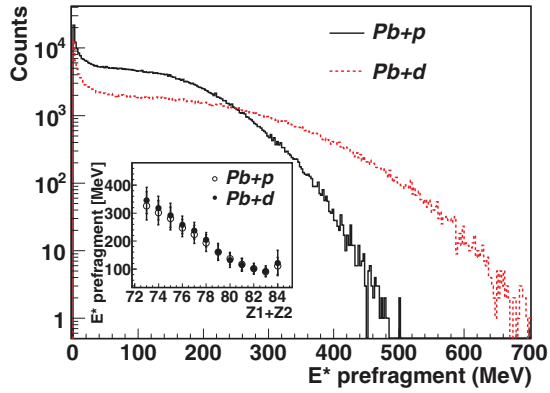

FIG. 6. (Color online) Distribution of the excitation energy gained by all the prefragments produced in the reactions ^{208}Pb + p (solid line) and ^{208}Pb + d (dotted line). Inset: Average excitation energy of the prefragments undergoing fission during the deexcitation stage as a function of $Z_1 + Z_2$ for the reactions ^{208}Pb + p (open circles) and ^{208}Pb + d (solid circles).

in reactions induced with protons (solid line). Since both distributions are normalized to the same number of counts, the figure reflects that the probability of producing pre-fragments with the largest excitation energies, and thus lower $Z_1 + Z_2$ values, is higher in the case of deuteron-induced reactions. In contrast, proton-induced reactions have larger probability of producing pre-fragments with lower excitation energy. This fact explains the difference in the partial fission cross sections between proton- and deuteron-induced reactions obtained for different values of $Z_1 + Z_2$.

We also show in the inset of Fig. 6 that, according to model calculations, there exists a clear correlation between $Z_1 + Z_2$ and the average excitation energy of the fissioning prefragments, as previously assumed. In addition, we also observe that the average excitation energy of the fissioning prefragments with a certain $Z_1 + Z_2$ value is similar for both reactions (open and solid circles for proton and deuteron, respectively), showing a small difference for the lowest $Z_1 + Z_2$ values because in the case of deuteron-induced reactions more neutrons are ejected on average.

In Fig. 7, we compare our partial fission cross sections with the charge distribution of spallation-evaporation residues obtained in Ref. [41] for the reaction ^{208}Pb + p at 500A MeV. The distribution of evaporation residues was normalized by a factor which corresponds to the ratio of the total evaporation cross sections (1.44 b) to the total fission cross section measured in the present work (149 mb). As can be seen, both distributions have a similar shape, however at higher excitation energies (lower $Z_1 + Z_2$) spallation-evaporation cross sections decrease faster than fission cross section. This deviation may appear owing to the influence of the competition between fissility and excitation energy determined during the deexcitation stage.

Figure 5 indicates that partial fission cross sections according to the total charge of the fissioning nucleus ($Z_1 + Z_2$) are sensitive to the entrance channel of the reaction. Therefore we can use this observable to constraint model calculations describing the prefragment formation in spallation reactions.

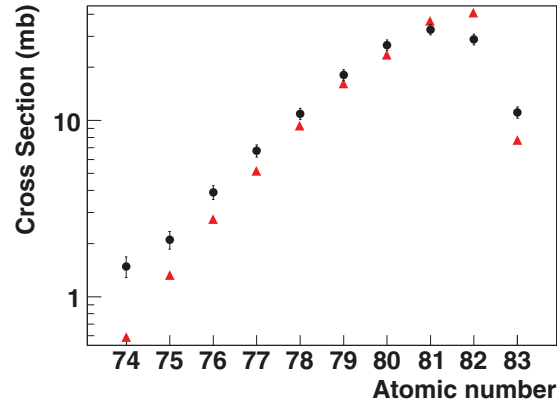

FIG. 7. (Color online) Partial fission cross sections (circles) and normalized cross sections of spallation-evaporation residues (triangles) for the reaction ^{208}Pb + p at 500A MeV [41]. The atomic number of the fissioning nucleus was determined by the sum $Z_1 + Z_2$.

Another observable studied in this work is the width of the fission fragments charge distributions (σ_z) as a function of the sum of the charges of the final fission fragments. According to a statistical interpretation, this observable should be proportional to the temperature of the fissioning system at the saddle point $T_{\rm sad}$ [42,43] according to the following expression:

$$\sigma_z^2 = Z_{\rm fis}^2 T_{\rm sad} / (16 d^2 V / d\eta^2) \qquad (1)$$

where $Z_{\rm fis}$ is the nuclear charge of the fissioning nucleus and $d^2V/d\eta^2$ is the stiffness of the potential with respect to the mass asymmetry $\eta = 4/A_{\rm fis}/(M - A_{\rm fis}/2)$. $A_{\rm fis}$ and M are the mass of the fissioning nuclei and the mass of the fragments, respectively. To establish the link between $T_{\rm sad}$ and σ_z, we used the stiffness of the potential parametrized as a function of the fissility proposed by Rusanov *et al.* [44]. It is worth mentioning that the variation of the potential with the fissility is relatively weak in the $Z_1 + Z_2$ range investigated in this work.

The results for the two reactions investigated in this work are shown in Fig. 8. As can be seen, the width of the charge

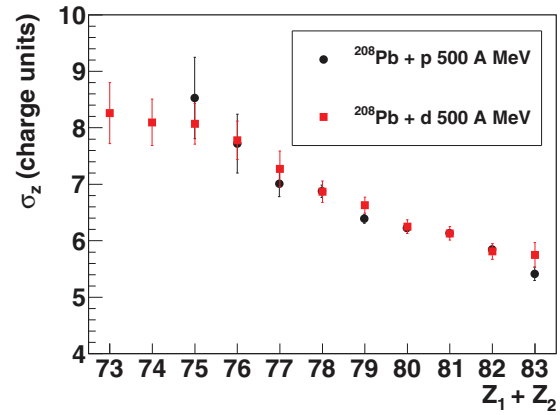

FIG. 8. (Color online) Width of the fission fragment charge distribution as a function of the charge of the fissioning nucleus for the reactions ^{208}Pb + p and ^{208}Pb + d at 500A MeV.

distribution increases when decreasing $Z_1 + Z_2$. This result confirms the expected increase of the width of the charge distribution of the fission fragments with the violence of the reaction. In addition, for both reactions we obtain very similar values of σ_z for each $Z_1 + Z_2$. We can conclude that this observable characterizes the compound fissioning system regardless of the target used to produce that fissioning nuclei. However, the range in $Z_1 + Z_2$ covered in each reaction is different because it reflects the initial excitation energy of the fissioning prefragments, which depends on the reaction entrance channel.

In summary, following the experimental technique proposed by Jurado *et al.* [6] and Schmitt *et al.* [7] we have used two observables characterizing the fissioning system at the initial configuration and at saddle. The partial fission cross sections according to the sum of the charges of the two fission fragments are sensitive to the entrance channel of the reaction. On the contrary, the evolution of the width of the charge distributions with the sum of the charges of the fission fragments does not seem to depend on the entrance channel. This result would support the relation of this observable with the temperature of the fissioning system at saddle. These two observables should then provide stringent constraints for model calculations describing the evolution of the fissioning system from the ground state to the saddle point [6,7].

B. Comparison to model calculations

To illustrate in a more quantitative way the sensitivity of these observables to dissipative and transient effects, reaction model calculations are needed. We have used INCL4.6 [45,46] and ISABEL [47] intranuclear cascade codes coupled to the deexcitation code ABLA07 [48]. A detailed description of these codes applied to proton-induced fission of ^{181}Ta at high excitation energies and to fragmentation reactions with spherical radioactive nuclei can be found in Refs. [21] and [7], respectively. Here, we will only remind their main features.

In intranuclear cascade codes, the collision of a high-energy projectile within a target nucleus initiates a succession of binary nucleon-nucleon collisions that may lead to the emission of pre-equilibrium nucleons. In INCL and ISABEL, nucleons are described as point-like particles, and as a continuous medium perturbed by the collisions induced by cascade particles, respectively. Nucleons in INCL are endowed within a realistic phase-space density (Woods-Saxon in configuration space, hard Fermi sphere in momentum space), while in ISABEL, both projectile and particle follow a folded Yukawa density distribution. In INCL, the excitation energy and the angular momentum induced by the intranuclear cascade are computed according to particle-hole excitations. The cascade stops self-consistently when the prefragment is assumed to be thermalized. In contrast, in ISABEL the cascade stops when the energy is below a specific cutoff energy. In both codes, the remaining excitation energy is distributed among all the nucleons.

The ABLA code describes the deexcitation of a thermalized compound nucleus by fission or by the emission of light charged particles, γ rays, neutrons and intermediate-mass fragments (IMF) following Weisskopf's model [49]. The

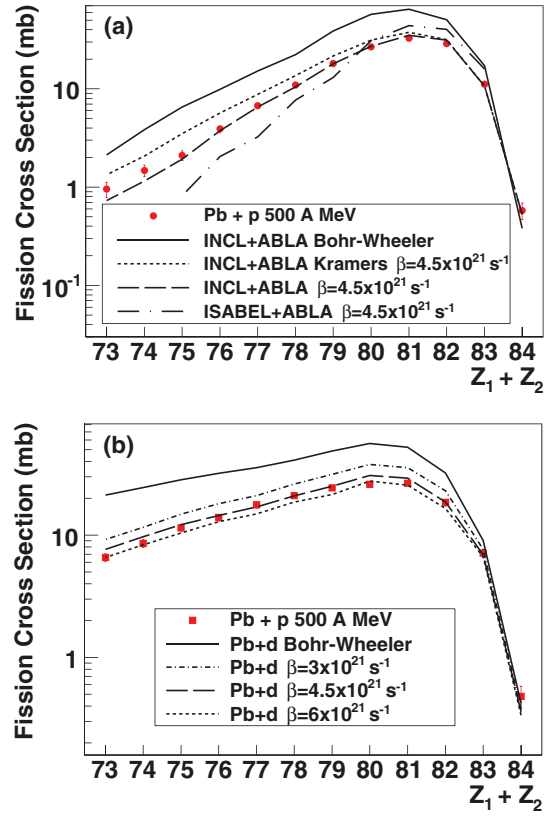

FIG. 9. (Color online) Upper panel: Comparison between model calculations performed with INCL and ISABEL coupled to ABLA, and the experimental partial fission cross sections (dots) for the reaction ^{208}Pb + p. Lower panel: Comparison between calculations performed with INCL + ABLA and partial fission cross sections for the reaction ^{208}Pb + d.

fission probability is computed according to a time-dependent fission width following the analytical description of the solutions of the corresponding Fokker-Plank equation proposed in Refs. [50–52]. The code also allows to evaluate the fission width according to the transition-state model of Bohr and Wheeler [8] or the time-independent formulation of Kramers [1]. Important parameters in the code are the level density parameters that are calculated according to the parametrization proposed by Ignatyuk [53] and angular momentum dependent fission barriers which are taken from Sierk's finite-range liquid drop model [54].

Results obtained with these model calculations are shown in Figs. 9 and 10. In the upper panel of Fig. 9 we benchmark calculations performed with INCL (dashed line) and ISABEL (dash-dotted line) coupled to the dynamical description of the fission process in ABLA for the reaction ^{208}Pb + p at 500A MeV with the partial fission cross sections measured in this work. As can be seen, the partial fission cross sections distribution can help to discriminate between spallation models. In this case, the shape of the partial fission cross sections should reflect the distribution of the initial excitation energy gained in the reaction. On the other hand, the absolute value of these cross sections should also reflect the fission probability of the prefragments. It has to be taken into account that

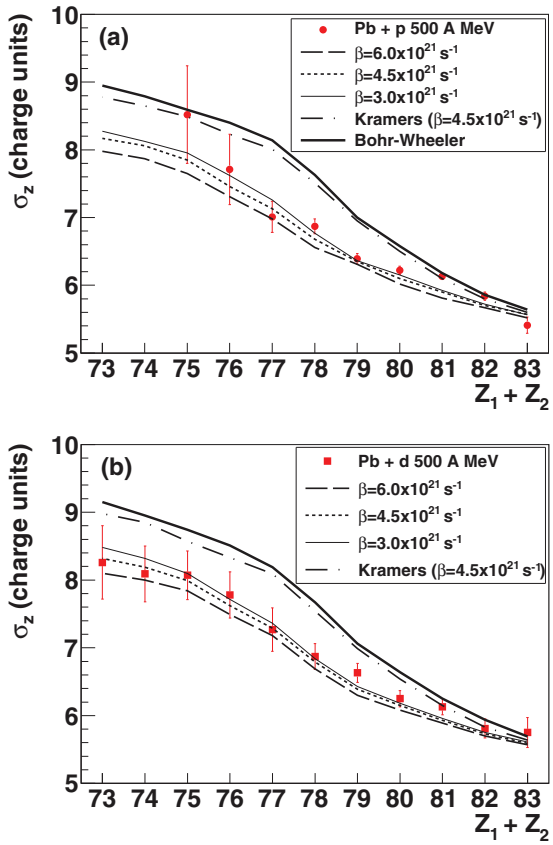

FIG. 10. (Color online) Calculations with INCL + ABLA compared to the experimental width of the fission fragment charge distribution (σ_z) as a function of the charge of the fissioning nucleus for ^{208}Pb + p (upper panel) and ^{208}Pb + d (lower panel) at 500A MeV.

total fission cross sections for the ^{208}Pb + p reaction at 500A MeV, calculated with INCL and ISABEL coupled to ABLA (with $\beta = 4.5 \times 10^{21}$ s^{-1}), amount to 144 and 156 mb, respectively. Therefore, despite this good agreement in the total fission cross section, the information inferred from the comparison of the partial fission cross sections with the calculations is more suitable to benchmark these codes. In conclusion, INCL provides a better agreement for the cross sections considering that ABLA includes a very realistic modellization of transient effects in the time dependence of the fission width benchmarked with a different entrance channel [55].

Partial fission cross sections can also be used to benchmark the model description of the fission process. Calculations with INCL + ABLA using the Bohr-Wheeler statistical model (solid lines) to describe fission clearly over-predict the experimental cross sections. For $Z_1 + Z_2$ values above 81, where fission takes place at lower excitation energy, time-dependent dynamical calculations considering a reduced dissipation strength of $\beta = 4.5 \times 10^{21}$ s^{-1} (dashed lines) and calculations according to the time-independent Kramers' model with the same value of β (dotted line) are in very good agreement with the data. The reason is that there exists an onset for the manifestation of transient effects [51] that depends on the excitation energy of the fissioning system and therefore on $Z_1 + Z_2$. Transient effects manifest only when the lifetime of the fissioning system becomes comparable to the time delay against fission induced by nuclear dissipation. We inferred from our model calculations an excitation energy threshold for the manifestation of transient effects of around 120 MeV for prefragments with $Z_1 + Z_2 = 81$, in good agreement with the result obtained in Ref. [21]. On the other hand, for $Z_1 + Z_2$ values lower than 81, where larger excitation energies are expected, time-dependent dynamical calculations better describe the measurements. Therefore, partial fission cross sections are sensitive to dynamical effects appearing in highly excited fissioning nuclei. It is also worth pointing out that the decrease of the fission cross section due to Kramer's fission width is also observed in the partial fission cross section spectrum in almost the whole range of $Z_1 + Z_2$ [7].

We also calculated partial fission cross sections for the reaction Pb + d using different values of the dissipation strength within the overdamped regime, characterized by an increase of the transient time with increasing β [51]. We observe in the lower panel of Fig. 9 that for $\beta = 3 \times 10^{21}$ s^{-1} (dotted line) and $\beta = 6 \times 10^{21}$ s^{-1} (dash-dotted line), model calculations are above and below the measured partial fission cross sections, respectively. The sensitivity of this observable to the dissipation strength allow us to determine an optimum value of $\beta = (4.5 \pm 1.0) \times 10^{21}$ s^{-1}.

We also investigated the role of nuclear dissipation in fission using the evolution of the widths of the fission fragments charge distribution as a function of $Z_1 + Z_2$. As previously mentioned, this observable provides information on the temperature of the fissioning system at the saddle. Again, we compared our measurements with calculations performed with INCL + ABLA (see Fig. 10). As can be seen, calculations according to the Bohr-Wheeler statistical model (thick solid line) predict σ_z values above the experimental ones, for values of $Z_1 + Z_2 < 80$. In contrast, dynamical calculations considering a dissipation strength of $\beta = 4.5 \times 10^{21}$ s^{-1} (dotted line) are in very good agreement with the experimental values obtained for ^{208}Pb + p and ^{208}Pb + d reactions. Therefore, the time-dependent fission width describing the partial fission cross sections also reproduces the widths of the charge distributions. The overall reduction of the width with respect to statistical calculations can be explained as follows: the fission delay induced by nuclear dissipation favors the deexcitation of the fissioning system by emitting particles and subsequently reducing its temperature at the saddle point. We also performed calculations using the time-independent Kramers fission width considering $\beta = 4.5 \times 10^{21}$ s^{-1} (dotted-dashed line) to emphasize that the reduction of σ_z is exclusively due to transient effects. While the stochastic behavior of the diffusion process induced by dissipation leads to a reduction of the fission width, and consequently of the cross section, only the time delay induced by dissipation reduces the temperature at the saddle point because the system has more time to evaporate particles along its way to the saddle [6,7,21]. For $Z_1 + Z_2 \geqslant 81$, all calculations are in good agreement with the experimental data. As stated before in the case of partial fission cross sections, for those $Z_1 + Z_2$ values corresponding to excitation energies of the prefragment below 120 MeV, the typical lifetime of the fissioning system is much larger than transient effects and we lose the sensitivity to the latter. From the calculations

we inferred a transient time of $1.2 \pm 0.4 \times 10^{-21}$ s. Finally, we also performed calculations for both reactions considering values of the dissipation strength of $\beta = 3.0 \times 10^{21}$ s^{-1} (thin solid line) and $\beta = 6.0 \times 10^{21}$ s^{-1} (dashed line). As expected, an increase (decrease) of the dissipation strength leads to slight decrease (increase) of σ_z. It can be also seen that this observable is less sensitive to the precise value of the nuclear viscosity, compared to partial fission cross sections. The sensitivity of the calculations to different β values within the overdamped regime is much weaker than in the case of partial fission cross sections because transient time increases slowly with the value of the nuclear dissipation strength. Taking into account the results of the calculations for both observables, we conclude a value for the dissipation strength of $\beta = (4.5 \pm 1.0) \times 10^{21}$ s^{-1}.

The results presented in this work are in good agreement with other experiments based on fragmentation [6,7,31] and spallation reactions [19–21] where highly excited fissioning nuclei were produced with small deformation. Concerning the reaction ^{238}U + CH_2 at 1A GeV investigated by Jurado *et al.* [6] we were also able to reproduce those data using a value for the dissipation strength of $\beta = 4.5 \times 10^{21}$ s^{-1} but including the initial deformation of the prefragments in the calculation of the fission width according to Ref. [48].

As conclusion, we investigated transient and dissipative effects in fission through two different observables sensitive to different stages of the fission process. The best description of the data was obtained when considering a time-dependent fission width with a value of the reduced dissipation coefficient $\beta = 4.5 \pm 0.5 \times 10^{21}$ s^{-1}. The intranuclear cascade allowed us to define the initial conditions of the fissioning system, taking into account that the shape of the partial fission cross section distribution depends on the production mechanism of the prefragment. On the other hand, from the deexcitation model parameters we inferred that the transient time governs the evolution of the system from ground to saddle. Despite these observables were already investigated in previous works [6,7], here we used simultaneously both observables to characterize the dynamics of fission using a reaction fulfilling the optimum conditions proposed for these investigations [3].

IV. SUMMARY AND CONCLUSIONS

In the present work we investigated proton- and deuteron-induced fission of ^{208}Pb at 500A MeV. A dedicated experimental setup adapted to measurements in inverse kinematics was used to unambiguously detect and identify both fission fragments in coincidence with high acceptance and efficiency. We reconstructed the charge of the fissioning system $Z_1 + Z_2$, which reflects the excitation energy gained in the reaction. We were also able to define two additional observables sensitive to dissipative and transient effects in fission. We determined with high precision the partial fission cross sections and the width of the fission-fragments charge distribution as a function of the atomic number of the fissioning system, for both reactions.

The evolution of the system was studied using both observables because they are sensitive to the formation and decay of the fissioning compound nuclei. Partial fission cross sections provide valuable information about the intranuclear cascade stage revealing that deuteron-induced fission leads to fissioning systems with higher excitation energy when compared to proton-induced fission at the same kinetic energy per nucleon. We suggest that the shape of the partial fission cross sections according to $Z_1 + Z_2$ reflects the excitation energy distribution of the prefragments produced during the intranuclear cascade. Concerning the width of the fission fragments charge distribution, we obtained consistent values for both reactions investigated in this work for all the $Z_1 + Z_2$ range but also with previous data obtained for similar fissioning nuclei. We conclude that this observable is only sensitive to the deexcitation mechanism, in particular to the temperature at the saddle point, because it does not depend on the entrance channel that rules the production of the prefragment.

In addition, we have compared the results obtained in this work with the theoretical predictions yielded by a combination of intranuclear cascade codes INCL and ISABEL coupled to the statistical code ABLA describing the deexcitation of the compound nucleus. This benchmark helped us to conclude that the INCL code provides a better description of the first stage of the reaction. We also conclude that a statistical description of the fission process according to the Bohr and Wheeler model overestimates both observables except for the largest values of $Z_1 + Z_2$ corresponding to the smallest values of excitation energy. However, calculations made with INCL + ABLA using a time-dependent description of the fission width are in good agreement with the experimental values obtained for the total and partial fission cross sections but also the width of the charge distribution of fission fragments, considering $\beta = (4.5 \pm 1.0) \times 10^{21}$ s^{-1}. A transient time of $1.2 \pm 0.4 \times 10^{-21}$ s is then needed to describe the experimental data. Therefore, this comparison of the experimental results with calculations performed with ABLA deexcitation code supports the manifestation of transient and dissipative effects on the fission process at high excitation energies.

For fission at lower excitation energies, we have shown that all calculations are in rather good agreement with the experimental data, probing that we are not sensitive to dissipative effects in that energy range. These results are consistent with other works showing the influence of transient and dissipative effects on the fission process through the same observables [6,7]. In conclusion, these two independent and consistent observables allowed us to characterize and describe the dynamical evolution of spherical fissioning systems between the ground state and the saddle point.

ACKNOWLEDGMENTS

This work was partially supported by the European Commission under the projects ANDES-FP7-249671 and CHANDA-FP7-605203, by the Spanish Ministry of Research and Innovation under the grants FPA2010-22174-C02-01, Consolider-CPAN-CSD 2007-00042, and BES-2008-005553, and by the Regional Government of Galicia under the program "grupos de referencia competitiva" 2013-11.

[1] H. A. Kramers, Physica **7**, 284 (1940).
[2] H. A. Weidenmüller, Prog. Part. Nucl. Phys. **3**, 49 (1980).
[3] P. Grangé, Li Jun-Qing, and H. A. Weidenmüller, Phys. Rev. C **27**, 2063 (1983).
[4] L. G. Moretto, K. X. Jing, R. Gatti, G. J. Wozniak, and R. P. Schmitt, Phys. Rev. Lett **75**, 4186 (1995).
[5] J. P. Lestone and S. G. McCalla, Phys. Rev. C **79**, 044611 (2009).
[6] B. Jurado, C. Schmitt, K. H. Schmidt, J. Benlliure, T. Enqvist, A. R. Junghans, A. Kelic, and F. Rejmund, Phys. Rev. Lett. **93**, 072501 (2004).
[7] C. Schmitt, K.-H. Schmidt, A. Kelić, A. Heinz, B. Jurado, and P. N. Nadtochy, Phys. Rev. C **81**, 064602 (2010).
[8] N. Bohr and J. A. Wheeler, Phys. Rev. **56**, 426 (1939).
[9] A. Gavron, J. R. Beene, B. Cheynis, R. L. Ferguson, F. E. Obenshain, F. Plasil, G. R. Young, G. A. Petitt, M. Jaaskelainen, D. G. Sarantites, and C. F. Maguire, Phys. Rev. Lett. **47**, 1255 (1981); **48**, 835(E) (1982).
[10] P. Fröbrich and I. I. Gontchar, Phys. Rep. **292**, 131 (1998).
[11] A. Gavron *et al.*, Phys. Rev. C **35**, 579 (1987).
[12] K. Siwek-Wilczynska, I. Skwira, and J. Wilczynski, Phys. Rev. C **72**, 034605 (2005).
[13] M. Thoennessen and G. F. Bertsch, Phys. Rev. Lett. **71**, 4303 (1993).
[14] Y. Aritomo, T. Wada, M. Ohta, and Y. Abe, Phys. Rev. C **59**, 796 (1999).
[15] K. X. Jing, L. W. Phair, L. G. Moretto, Th. Rubehn, L. Beaulieu, T. S. Fan, and G. J. Wozniak, Phys. Lett. B **518**, 221 (2001).
[16] D. J. Hinde, D. Hilscher, H. Rossner, B. Gebauer, M. Lehmann, and M. Wilpert, Phys. Rev. C **45**, 1229 (1992).
[17] D. Hilscher and H. Rossner, Ann. Phys. Fr. **17**, 471 (1992).
[18] J. Benlliure *et al.*, Nucl. Phys. A **683**, 513 (2001).
[19] J. Benlliure, E. Casarejos, J. Pereira, and K.-H. Schmidt, Phys. Rev. C **74**, 014609 (2006).
[20] J. Benlliure *et al.*, Nucl. Phys. A **700**, 469 (2002).
[21] Y. Ayyad *et al.*, Phys. Rev. C **89**, 054610 (2014).
[22] R. Serber, Phys. Rev. **72**, 1114 (1947).
[23] M. de Jong, A. V. Ignatyuk and K.-H. Schmidt, Nucl. Phys. A **613**, 435 (1997).
[24] W. Ye and N. Wang, Phys. Rev. C **86**, 034605 (2012).
[25] K. H. Bhatt, P. Grangé, and B. Hiller, Phys. Rev. C **33**, 954 (1986).
[26] R. L. Folger, P. C. Stevenson, and G. T. Seaborg, Phys. Rev. **98**, 107 (1955).
[27] B. Foreman, W. Gibson, R. Glass, and G. Seaborg, Phys. Rev. **116**, 382 (1959).
[28] S. Regnier, M. Baklouti, M. Simonoff-Lagarde, and G. N. Simonoff, Phys. Lett. B **68**, 202 (1977).
[29] L. A. Vaishnene, V. G. Vovchenko, Yu. A. Gavrikov, A. A. Kotov, V. I. Murzin, V. V. Poliakov, M. G. Tverskoy, O. Ya. Fedorov, Yu. A. Chestnov, A. V. Shvedchikov, and A. I. Shchetkovskii, Bull. Russ. Acad. Sci. Phys. **74**, 496 (2010).
[30] K. H. Schmidt *et al.*, Nucl. Phys. A **665**, 221 (2000).
[31] C. Schmitt, P. N. Nadtochy, A. Heinz, B. Jurado, A. Kelic, and K.-H. Schmidt, Phys. Rev. Lett. **99**, 042701 (2007).
[32] K. H. Schmidt *et al.*, Phys. Rev. C **87**, 034601 (2013).
[33] J. L. Rodríguez-Sánchez *et al.*, Phys. Rev. C **90**, 064606 (2014).
[34] A. Kelić *et al.*, Phys. Rev. C **70**, 064608 (2004).
[35] J. C. David, A. Boudard, J. Cugnon, S. Ghali, S. Leray, D. Mancusi, and L. Zanini, Eur. Phys. J. A **49**, 29 (2013).
[36] A. Heinz *et al.*, Nucl. Phys. A **713**, 3 (2003).
[37] B. Fernández *et al.*, Nucl. Phys. A **747**, 227 (2005).
[38] E. Hagebø and T. Lund, J. Inorg. Nucl. Chem. **37**, 1569 (1975).
[39] T. Enqvist *et al.*, Nucl. Phys. A **703**, 435 (2002).
[40] D. Tarrío *et al.*, Phys. Rev. C **83**, 044620 (2011).
[41] L. Audouin *et al.*, Nucl. Phys. A **768**, 1 (2006).
[42] P. Fong, *Statistical Theory of Nuclear Fission* (Cordon and Breach, New York, 1969).
[43] M. G. Itkis, V. N. Okolovich, A. Ya. Rusanov, and G. N. Smirenkin, Sov. J. Part. Nucl. **19**, 301 (1988).
[44] A. Ya. Rusanov, M. G. Itkis, and V. N. Okolovic, Phys. At. Nucl. **60**, 773 (1997).
[45] J. Cugnon, C. Volant, and S. Vuillier, Nucl. Phys. A **620**, 475 (1997).
[46] A. Boudard, J. Cugnon, J.-C. David, S. Leray, and D. Mancusi, Phys. Rev. C **87**, 014606 (2013).
[47] Y. Yariv and Z. Fraenkel, Phys. Rev. C **20**, 2227 (1979).
[48] A. Kelic, M. V. Ricciardi, and K.-H. Schmidt, in *Proceeding of Joint ICTP-IAEA Advanced Workshop on Model Codes for Spallation Reactions, ICTP Trieste, Italy, 4–8 February, 2008*, edited by D. Filges, S. Leray, Y. Yariv, A. Mengoni, A. Stanculescu, and G. Mank (IAEA, Vienna, 2008), INDC(NDS)-530, pp. 181–221.
[49] V. Weisskopf, Phys. Rev. **52**, 295 (1937).
[50] B. Jurado, K.-H. Schmidt, and J. Benlliure, Phys. Lett. B **533**, 186 (2003).
[51] B. Jurado, C. Schmitt, K.-H. Schmidt, J. Benlliure, and A. R. Junghans, Nucl. Phys. A **747**, 14 (2005).
[52] B. Jurado, C. Schmitt, K.-H. Schmidt, J. Benlliure, and A. R. Junghans, Nucl. Phys. A **757**, 329 (2005).
[53] A. V. Ignatyuk *et al.*, Sov. J. Nucl. Phys. **21**, 612 (1975).
[54] A. J. Sierk, Phys. Rev. C **33**, 2039 (1986).
[55] J. J. Gaimard and K. H. Schmidt, Nucl. Phys. A **531**, 709 (1991).